

Draft 6 – For submission to Nature

Thursday, January 24, 2002

Contrasting rates and scales of sediment production and sediment yield in semi-arid terrain

Paul R. Bierman^a, Milan Pavich^b, Allen Gellis^b, Marc W. Caffee^c, and Jennifer Larsen^a

^aGeology Department and School of Natural Resources, University of Vermont,
Burlington, VT 05405

^bUnited States Geological Survey, National Center, Reston, VA, 22092

^cCenter for Accelerator Mass Spectrometry, Lawrence Livermore National Laboratory,
Livermore, CA 94550; now at: PRIME Laboratory, Physics Department, Purdue
University, West Lafayette, IN 47907

**The rates at which sediment is generated on hillslopes by weathering
(sediment production) and exported from drainage basins by rivers (sediment yield)
are highly variable, poorly known, and difficult to predict^{1,2}; yet, quantifying such
rates over space and time is fundamental to understanding the behavior of Earth's
surface, linking surficial and deep-Earth processes³⁻⁵, and placing human impact in
sufficient context for the development of informed land-management strategies.
Semi-arid regions are of particular concern because they have some of the highest
sediment yields in the world⁶ and because their populations are growing rapidly⁷.
Here, using in-situ-produced ¹⁰Be measured in 52 alluvial sediment samples**

collected from the 16,000 km² drainage network of Rio Puerco Basin of northern New Mexico, we show that rates of sediment export and rates of sediment production vary over significantly different temporal and spatial scales. We demonstrate that cosmogenic nuclides provide a rapid means by which to determine rates and patterns of sediment generation even in large basins with significant, albeit short-term, sediment storage.

Suspended sediment concentrations in the Rio Puerco, the largest tributary of the Rio Grande, are among the highest in the world⁸ (up to 600,000 mg/l; Fig. 1). Steep, forested headwaters with thin soils and frequent bare rock mesas are underlain by a variety of lithologies including sandstone, shale, and volcanic rocks; the highlands stand in stark contrast to the grass-covered, alluviated valley bottoms (Fig. 2). At present, much of the alluvial drainage network is deeply incised, the result of an arroyo-cutting episode that began in the late 1800s⁹. Although the cause of arroyo incision here and throughout southwestern North America is uncertain (arroyos have been attributed to both natural cycles and the impact of livestock grazing¹⁰), the geomorphic and societal impacts of arroyo incision were and are dramatic⁹. Large volumes of unconsolidated sediment are delivered directly to the channel by a combination of geomorphic processes including scour, head cutting, and bank collapse as channels widen and deepen¹¹. Young radiocarbon ages, and the lack of identifiable paleosols in most arroyo walls, demonstrate

that cutting and filling of Rio Puerco arroyos have occurred repeatedly during the Holocene on millennial timescales^{12,13}.

To determine the rate at which sediment is generated by rock weathering on hillslopes, to test the relationship between ¹⁰Be activity in fluvial sediment and drainage basin area, and to compare long-term rates of sediment production (monitored with ¹⁰Be) with short term rates of sediment export (calculated from suspended sediment load), we collected and measured ¹⁰Be in sand-sized (250 to 850 μm) alluvial sediment from 37 sites in the channel within the boundaries of the 20th century arroyos (Fig 1; Table A, Supplementary data). Drainage basin areas above sample sites ranged from 170 km² to 16,000 km². Sixteen samples were collected from headwater basins; the other samples were collected farther downstream in higher-order channels. We also collected a depth profile of 15 samples and four pieces of charcoal for ¹⁴C dating (Table B, Supplementary data) from sediment exposed in a 6-m high arroyo wall to test for the consistency of ¹⁰Be activity in fluvial sediment over time. We separated quartz from the samples and isolated ¹⁰Be using standard techniques¹⁴. Ratios of ¹⁰Be/⁹Be were measured by accelerator mass spectrometry at Livermore National Laboratory.

To calculate rates of sediment generation from ¹⁰Be measured in Rio Puerco alluvium, we used an interpretive, analytical model that relates nuclide activity in fluvial sediment to the rate at which drainage basins are eroding and producing sediment¹⁵⁻¹⁷.

This model had previously been applied primarily to small headwater basins where the

assumptions of thorough sediment mixing, minimal sediment storage time, and uniform nuclide production rates were most likely to be met^{14,16,18-21}. To calculate effective nuclide production rates for each Rio Puerco sub-basin¹⁵, we convolved DEM-generated hypsometry (100 m bins) with the altitude-production rate function²² assuming a sea-level, high-latitude ¹⁰Be production rate²³ of 5.17 atoms g⁻¹ y⁻¹.

Rio Puerco data demonstrate that in-situ-produced ¹⁰Be can be a useful monitor of sediment generation in both small and large basins (Table A, Supplementary Data, is available). Individual basin-scale rates of sediment generation range from 1.9 * 10⁴ kg km² y⁻¹ to 9.2 * 10⁵ kg km² y⁻¹, the equivalent of rock erosion at 7 to 355 m My⁻¹ ($\rho = 2600 \text{ kg m}^3$). Scatter in modeled rates of sediment generation is higher for smaller basins (<2000 km²) than for larger basins but variability dampens with increasing basin area, demonstrating the importance and efficiency of sediment mixing during fluvial transport. The variability in nuclide activity between samples from small basins (Fig. 3) suggests that basin-to-basin differences in slope, precipitation, and lithology influence erosion rates and thus nuclide activity at headwater scales.

The basin-area average sediment generation rate (2.4*10⁵ kg km² y⁻¹) determined from a single sample (RP-5) collected just below the confluence of the Rio Puerco's two main tributaries (drainage area, 14,200 km²) is similar to the area-weighted average sediment generation rate (2.9 *10⁵ kg km² y⁻¹) calculated from the 15 headwater basins (average drainage area, 495 km²), upstream of RP-5. This finding implies that sediment

is mixed well as it moves from eroding headwaters through the drainage network even in a basin of this scale and even with the sporadic flow events that characterize this semiarid region. We can detect no downstream increase in nuclide activity; thus, sediment is conveyed with sufficient rapidity that storage in the valley-bottom, and the nuclides accumulated during such storage, do not add significantly to initial nuclide activity generated during weathering on and detachment from hill slopes. Together, the nuclide data show that uplands in the Rio Puerco Basin are lowering on average about 100 m My^{-1} , consistent with values determined by several other methods^{8,18}.

Nuclide activity in sediment transported by the Rio Puerco does not appear to have changed significantly over the Holocene (Fig. 4). Fifteen samples from an arroyo wall exposed by channel incision in the late 19th century have similar ^{10}Be activities ($1.08 \pm 0.10 * 10^5 \text{ atom g}^{-1}$) despite being deposited over more than a millennium in at least two cut and fill cycles. This critical observation, along with the buffering implied by the meter-scale depth of cosmic ray penetration¹⁵ and the $\sim 100 \text{ m My}^{-1}$ erosion rate, suggest that ^{10}Be activity measured in 20th century alluvium represents rates of sediment generation integrated over much, if not all, of the Holocene. ^{10}Be activity in the arroyo wall is within the range of values measured for modern alluvium upstream and downstream of sampling site (RP -22, -23, -27, and -21; range = 0.99 to $1.25 * 10^5 \text{ atom g}^{-1}$). Thus, when arroyo walls collapse, they deliver sediment to the channel with nuclide activity indistinguishable from that of sediment in transit. Such similarity results directly

from the rapid cycle of arroyo cutting and filling that minimizes cosmic-ray dosing during storage of the thick alluvial packages. Both radiocarbon ages and the ^{10}Be analysis suggest that average sediment storage times in Rio Puerco valley bottoms are short, on the order of no more than a few thousand years.

Sediment generation rates in the Rio Puerco Basin are less than contemporary (1948-1956) rates of sediment yield. Suspended sediment records collected at USGS stations in six basins (1 to 16,000 km²) show that sediment is currently being removed from the basin faster than it is being generated (Fig. 5). Such disparity is driven by the arroyo cycle. During periods when arroyos are incising, sediment is removed from temporary valley-bottom storage and sediment yield exceeds rates of sediment generation. Conversely, during periods when arroyos are filling, sediment yield must be less than the rate of sediment generation as the volume of sediment in storage increases. The removal of sediment from valley bottom storage and the disparity between sediment production rates (^{10}Be) and sediment yield (suspended sediment data) indicate that over human timescales the basin is not in steady-state; yet, over longer time scales, the repeated cutting and filling of arroyos and the similarity of ^{10}Be activity throughout the arroyo wall profile suggest that sediment production and yield are indeed in balance.

Our results suggest an underlying dynamic equilibrium over the Holocene of upland sediment production, delivery, and short-term storage in valley fills followed by repeated, episodic arroyo incision and alluvium reworking by the Rio Puerco and its

tributaries. The combination of easily eroded lithologies, sparse vegetation, and monsoon-dominated rainfall result in rapid sediment generation and efficient sediment delivery from tributaries to the main Puerco channel. Measurements of ^{10}Be establish a background rate of sediment production that appears to have changed little over the Holocene.

Data presented here demonstrate that in-situ-produced cosmogenic nuclides have the potential to provide rapid assessment of sediment generation rates not only in small, homogeneous basins^{16,17,19} but also over a wide range of tributary areas, lithologies, and vegetation covers. However, in semi-arid, southwestern North America, the cycling of arroyos on millennial time scales suggests that such a background rate of sediment generation has little predictive value in terms of sediment yield, often a benchmark parameter for evaluating the efficacy of land management strategies. As arroyos cut and fill, sediment yields are time-scale dependent while sediment generation rates on hillslopes, as tracked by ^{10}Be activity, change little. This time-dependent variability in sediment yield and thus background rates of stream water turbidity suggests that any regulatory framework for suspended sediment in arid and semi-arid streams and rivers consider natural, time-dependent changes in sediment concentration.

Figure Captions

Figure 1. Rio Puerco drainage network and locations (solid circles) of alluvial sediment samples collected for ^{10}Be analysis; location of sampled arroyo wall (RP-22a) shown by arrow. Solid boxes indicate stations where suspended sediment data were collected. Inset is digital elevation model of New Mexico; study area outlined in black.

Figure 2. Air photograph of Rio Puerco at sample site RP-21; incised arroyo in foreground and bedrock slopes at margin. Road in lower left for scale.

Figure 3. Sediment production rates, expressed as rates of rock erosion ($\rho = 2600 \text{ kg m}^{-2}$), are more variable for small basins than for larger basins demonstrating the efficacy of mixing during fluvial transport.

Figure 4. ^{10}Be activity of 15 samples collected from arroyo wall near sample site RP-22 show little change in nuclide activity of deposited sediment. ^{14}C ages on charcoal shown on right side of graph with 1σ counting uncertainty (supplemental Table B). All but lowermost sample age are inseparable at 2σ . Solid vertical line is mean ^{10}Be activity ($n = 15$); dashed vertical lines are 1σ about the mean. Four samples have nuclide activity more than 1σ greater or less than the column average. These outliers have nuclide activity similar to that measured in the large

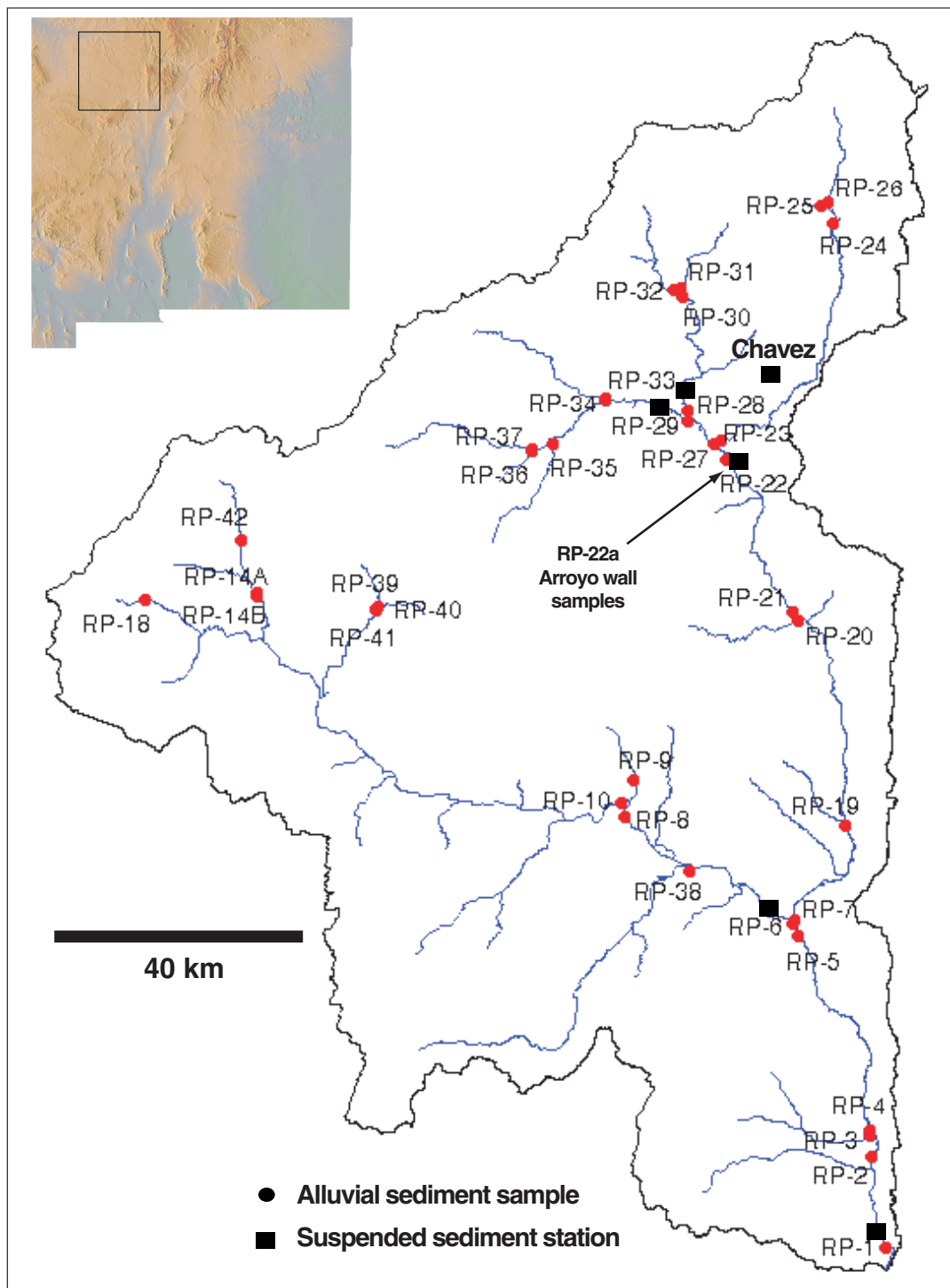
tributaries which join just above the sample site (RP-23, -27, -28, and -29) and most likely represent sediment contributed in spatially restricted runoff events affecting one or more, but not all, tributaries.

Figure 5. Comparison of suspended sediment yield (USGS data, 1948-1956, available from http://climchange.cr.usgs.gov/rio_puerco/erosion/streamflow.html) and ^{10}Be -derived sediment production estimates ($r^2=0.53$; $y = 1.5x + 45$), dashed regression line). Sample number and basin area plotted next to samples. Chavez refers to previously published data for small watershed¹⁸. Station names are: RP-23, Rio Puerco above Chico; RP-4 Rio Puerco at Puerco; RP-29 Arroyo Chico; RP-1 Rio Puerco at Bernardo; RP-6 Rio San Jose.

References Cited

1. Saunders, I. & Young, A. Rates of surface processes on slopes, slope retreat, and denudation. *Earth Surface Processes and Landforms* **8**, 473-501 (1983).
2. Milliman, J. D. & Meade, R. H. Worldwide delivery of river sediment to the oceans. *Journal of Geology* **91**, 1-21 (1983).
3. Adams, J. Contemporary uplift and erosion of the Southern Alps, New Zealand. *Geological Society of America Bulletin Part II*, v. **91**, 1-114 (1980).
4. England, P. Metamorphic pressure estimates and subsequent volumes for Alpine orogeny: an independent control on geobarometers? *Earth and Planetary Science Letters* **56**, 387-397 (1981).
5. Pazzaglia, F. J. & Brandon, M. T. A fluvial record of long-term steady state uplift and erosion across the Cascadia Forearc High, western Washington State. *American Journal of Science* **301**, 385-431 (2001).
6. Langbein, W. D., and Schumm, S.A. Yield of sediment in relation to mean annual precipitation. *Transactions of the American Geophysical Union* **39**, 1076-1084 (1958).
7. United Nations Population Fund. State of World Population. (2001).
8. Gellis, A. C., Pavich, M. J. & Ellwein, A. in *Proceedings of the 7th Federal Interagency Sedimentation Conference V* 83-91 (2001).
9. Bryan, K. Date of channel trenching in the arid Southwest. *Science* **62**, 338-344 (1925).
10. Cooke, R. U. & Reeves, R. W. *Arroyos and Environmental Change in the American South-West* (Clarendon Press, Oxford, 1976).
11. Elliott, J. G., Gellis, A. C. & Aby, S. B. in *Incised Channels--Processes, Forms, Engineering and Management* (ed. Darby, S. E., and Simon, A.) 153-185 (1999).
12. Love, D. W. in *IAHS Publication* (ed. Hadley, R. F.) 305-322 (1986).
13. Pavich, M. J., Gellis, A. C. & Aby, S. Chronostratigraphy of Quaternary alluvium, Rio Puerco basin, New Mexico. *Geological Society of America Abstracts with Program* **27**, A-372 (1997).
14. Bierman, P. R. & Caffee, M. W. Steady state rates of rock surface erosion and sediment production across the hyperarid Namib desert and the Namibian escarpment, southern Africa. *American Journal of Science* **301**, 326-358 (2001).
15. Bierman, P. & Steig, E. Estimating rates of denudation and sediment transport using cosmogenic isotope abundances in sediment. *Earth Surface Processes and Landforms* **21**, 125-139 (1996).
16. Granger, D. E., Kirchner, J. W. & Finkel, R. Spatially averaged long-term erosion rates measured from in-situ produced cosmogenic nuclides in alluvial sediment. *Journal of Geology* **104**, 249-257 (1996).

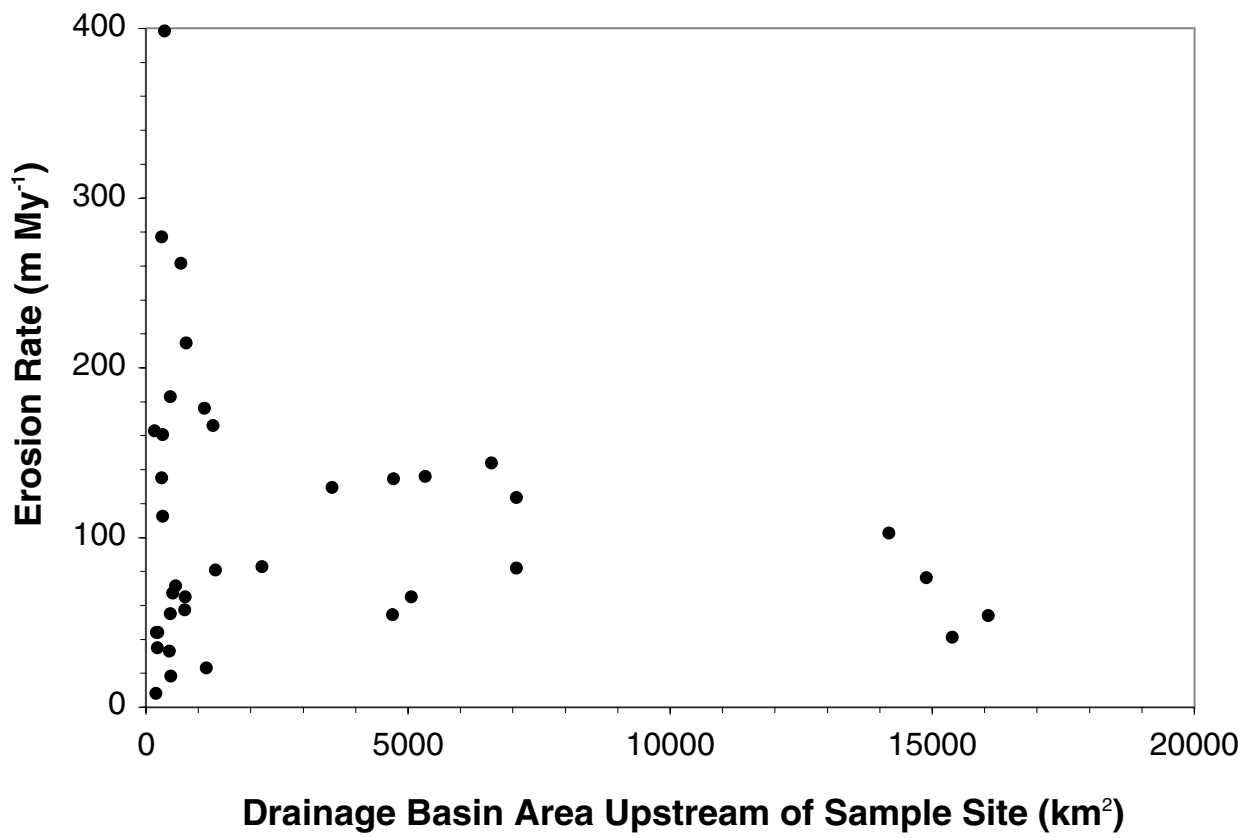
17. Brown, E., Stallard, R. F., Larsen, M. C., Raisbeck, G. M. & Yiou, F. Denudation rates determined from the accumulation of in situ-produced ^{10}Be in the Luquillo Experimental Forest, Puerto Rico. *Earth and Planetary Science Letters* **129**, 193-202 (1995).
18. Clapp, E., Bierman, P. R., Pavich, M. & Caffee, M. Rates of sediment supply to arroyos from uplands determined using in situ produced cosmogenic ^{10}Be and ^{26}Al in sediments. *Quaternary Research* **55**, 235-245 (2001).
19. Clapp, E. M. et al. Differing rates of sediment production and sediment yield. *Geology* **28**, 995-998 (2000).
20. Clapp, E., Bierman, P. R. & Caffee, M. Using ^{10}Be and ^{26}Al to determine sediment generation rates and identify sediment source in an arid region drainage basin. *Geomorphology* (in press).
21. Bierman, P., Clapp, E. M., Nichols, K. K., Gillespie, A. R. & Caffee, M. in *Landscape Erosion and Evolution Modeling* (eds. Harmon, R. S. & Doe, W. M.) 89-116 (Kluwer, New York, 2001).
22. Lal, D. Cosmic ray labeling of erosion surfaces: *In situ* production rates and erosion models. *Earth and Planetary Science Letters* **104**, 424-439 (1991).
23. Bierman, P., Larsen, P., Clapp, E. & Clark, D. Refining estimates of ^{10}Be and ^{26}Al production rates. *Radiocarbon* **38**, 149 (1996).
24. Research supported by USGS and National Science Foundation. B. Copans assisted with sample preparation. E.A. Cassell and E. Clapp assisted with sample collection.



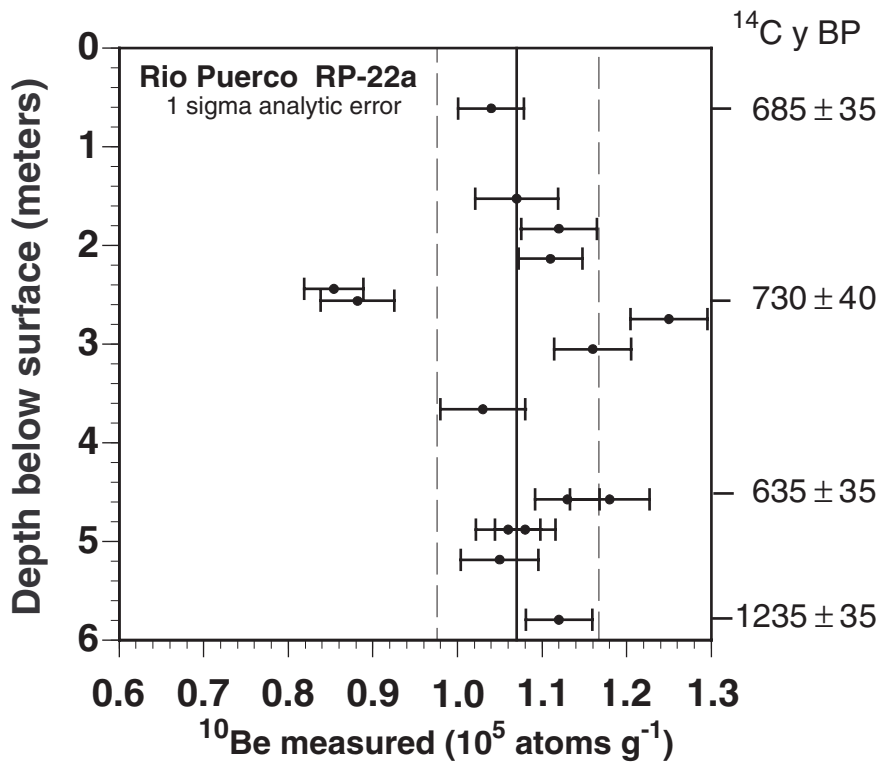
Bierman et al. Figure 1



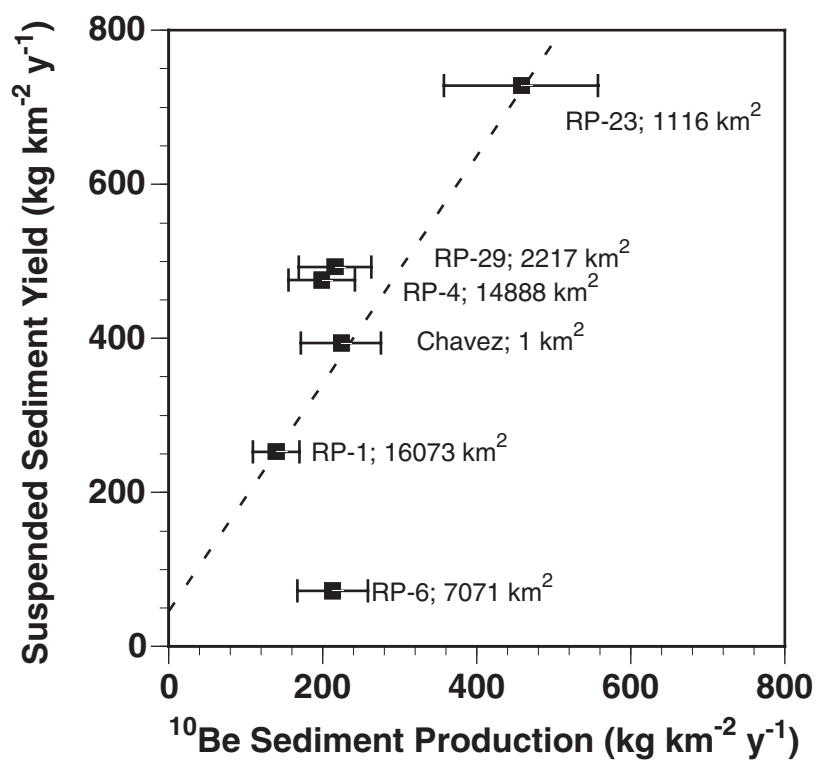
Bierman et al. Figure 2



Bierman et al. Figure 3



Bierman et al. Figure 4



Bierman et al. Figure 5

SUPPLEMENTAL DATA: TABLE A. Cosmogenic data for Rio Puerco sediment samples

Type ¹	Sample	Weighted Nuclide Production Factor ²	Basin Area km ²	¹⁰ Be Measured ³ (10 ⁵ atom g ⁻¹)	¹⁰ Be (SL, >60°) ⁴ (10 ⁵ atom g ⁻¹)	¹⁰ Be model sediment generation (10 ⁵ kg km ² y ⁻¹)	¹⁰ Be model ε ⁵ (m My ⁻¹)
	RP-01	4.28	16073	2.90 ± 0.09	0.678 ± 0.020	1.25 ± 0.15	48 ± 6
	RP-02	4.33	15385	3.82 ± 0.11	0.884 ± 0.026	0.96 ± 0.12	37 ± 5
HW	RP-03	3.58	473	7.08 ± 0.21	1.981 ± 0.060	0.42 ± 0.05	16 ± 2
	RP-04	4.35	14888	2.09 ± 0.07	0.481 ± 0.015	1.77 ± 0.22	68 ± 8
	RP-05	4.41	14177	1.58 ± 0.05	0.358 ± 0.012	2.38 ± 0.29	91 ± 11
	RP-06	4.55	7071	2.04 ± 0.07	0.448 ± 0.015	1.90 ± 0.23	73 ± 9
	RP-07	4.28	7071	1.27 ± 0.05	0.298 ± 0.012	2.86 ± 0.35	110 ± 13
	RP-08A	4.76	5063	2.69 ± 0.08	0.565 ± 0.017	1.50 ± 0.18	58 ± 7
HW	RP-09	5.10	323	1.17 ± 0.07	0.229 ± 0.014	3.72 ± 0.46	143 ± 18
	RP-10	4.74	4706	3.17 ± 0.16	0.670 ± 0.034	1.27 ± 0.16	49 ± 6
HW	RP-14	4.76	742	3.04 ± 0.09	0.639 ± 0.019	1.33 ± 0.16	51 ± 6
	RP-14B	4.76	748	2.68 ± 0.08	0.563 ± 0.017	1.51 ± 0.19	58 ± 7
	RP-18	5.55	191	24.00 ± 0.59	4.332 ± 0.107	0.19 ± 0.02	7 ± 1
	RP-19	4.34	6592	1.11 ± 0.04	0.255 ± 0.009	3.33 ± 0.41	128 ± 16
HW	RP-20	4.36	303	1.18 ± 0.04	0.272 ± 0.009	3.13 ± 0.38	120 ± 15
	RP-21	4.49	5328	1.21 ± 0.06	0.270 ± 0.014	3.15 ± 0.39	121 ± 15
	RP-22	4.52	4725	1.24 ± 0.05	0.273 ± 0.011	3.11 ± 0.38	120 ± 15
	RP-23	4.76	1116	0.99 ± 0.05	0.209 ± 0.010	4.08 ± 0.50	157 ± 19
	RP-24	5.13	666	0.72 ± 0.04	0.141 ± 0.007	6.06 ± 0.74	233 ± 29
	RP-25	4.59	169	1.04 ± 0.05	0.226 ± 0.010	3.77 ± 0.46	145 ± 18
HW	RP-26	5.35	359	0.49 ± 0.03	0.092 ± 0.006	9.22 ± 1.13	355 ± 43
	RP-27	4.45	3552	1.26 ± 0.05	0.284 ± 0.012	3.00 ± 0.37	115 ± 14
	RP-28	4.26	1283	0.94 ± 0.04	0.221 ± 0.009	3.84 ± 0.47	148 ± 18
	RP-29	4.56	2217	2.02 ± 0.07	0.443 ± 0.016	1.92 ± 0.24	74 ± 9
	RP-30	4.35	770	0.74 ± 0.03	0.171 ± 0.008	4.97 ± 0.61	191 ± 23
HW	RP-31	4.35	301	0.58 ± 0.03	0.133 ± 0.007	6.42 ± 0.79	247 ± 30
HW	RP-32	4.35	464	0.87 ± 0.04	0.201 ± 0.010	4.23 ± 0.52	163 ± 20
	RP-33	4.26	570	2.19 ± 0.08	0.514 ± 0.018	1.65 ± 0.20	64 ± 8
HW	RP-34	4.70	1326	2.13 ± 0.08	0.454 ± 0.017	1.87 ± 0.23	72 ± 9
	RP-35	5.20	464	3.44 ± 0.11	0.663 ± 0.022	1.28 ± 0.16	49 ± 6
HW	RP-36	4.53	206	3.75 ± 0.13	0.830 ± 0.028	1.02 ± 0.13	39 ± 5
HW	RP-37	4.49	510	2.45 ± 0.09	0.546 ± 0.020	1.55 ± 0.19	60 ± 7
HW	RP-38	4.10	1150	6.40 ± 0.18	1.561 ± 0.045	0.54 ± 0.07	21 ± 3
HW	RP-39	4.68	227	3.88 ± 0.14	0.830 ± 0.031	1.02 ± 0.13	39 ± 5
HW	RP-40	5.35	224	5.58 ± 0.21	1.044 ± 0.040	0.81 ± 0.10	31 ± 4
	RP-41	5.01	451	5.55 ± 0.23	1.108 ± 0.046	0.76 ± 0.09	29 ± 4
HW	RP-42	4.88	323	1.59 ± 0.06	0.326 ± 0.012	2.61 ± 0.32	100 ± 12

Notes

¹ HW= headwater drainage basin; no samples collected upstream.

² calculated by convolving drainage basin hypsometry (100 m elevation bins) with elevation/latitude production rate model of Lal (1991) considering only neutron-induced production.

³ Uncertainties in atomic abundances (1σ) represent quadratic addition of the error associated with the AMS ratio measurement as determined by the larger of the internal (counting statistics) and external (replication) errors, the 1σ uncertainty in Be carrier addition (2%) . These results are corrected for ratios measured in process blanks.

⁴ calculated using weighted nuclide production factor

⁵ Uncertainties in erosion rates are fully propagated from AMS uncertainties and include a 10% 1σ uncertainty in nuclide production rates including scaling factors for altitude and latitude, as well as 5% 1σ uncertainties in density, attenuation coefficients, and half-lives. Density of 2.6 g cm⁻³ assumed.

SUPPLEMENTAL DATA: TABLE B. Radiocarbon Dates, Arroyo Wall Exposure

CAMS #	Depth below surface (m)	Sample Name	¹⁴C age (yr)
81530	0.61	RP 22A 2'	685 ± 35
81532	2.56	RP 22A 8.4'	730 ± 40
81533	4.57	RP 22B 15'	635 ± 35
81534	5.79	RP 22B 19'	1235 ± 35

Notes:

Age in radiocarbon years using the Libby half life of 5568 years and measured ¹³C values. Sample preparation backgrounds have been subtracted, based on measurements of samples of 14C-free coal. Backgrounds scaled relative to sample size.